AD-787 745

DEVELOPMENT OF AN INTERNAL WAVE COMPUTER CODE

Patrick J. Roache, et al

Science Application, Incorporated

Prepared for:

Office of Naval Research
Advanced Research Projects Agency
Flow Research, Incorporated

1974

DISTRIBUTED BY:

NTIS
National Technical Information Service
U. S. DEPARTMENT OF COMMERCE

AD 787 745

SAI-74-648-LJ
30 October 1974

DEVELOPMENT OF AN INTERNAL WAVE COMPUTER CODE

James A. Young, Principal Investigator {(714) 459-0211}
Patrick J. Roache
Cyril W. Hirt
Science Applications, Inc.

Robert E. Robins
James J. Riley
Flow Research, Inc.

DDC
NOV 4 1974
C

Covering the Period 1 August 1974 through 31 October 1974

Sponsored by
Advanced Research Projects Agency
ARPA Order No. 1910

NR 062-496

Program Code No. 4E20
Contract Effective 15 March 1974, Expiration 15 July 1975
Contract Amount $215,943.00
Contract N00014-74-C-0340
Scientific Officer: Director Fluid Dynamics Programs, Office of Naval Research

The views and conclusions contained in this document are those of the authors and should not be interpreted as necessarily representing the official policies, either expressed or implied, of the Advanced Research Projects Agency or the U. S. Government.

SCIENCE APPLICATIONS, LA JOLLA, CALIFORNIA, Contractor
ALBUQUERQUE • ANN ARBOR • ARLINGTON • ATLANTA • BOSTON • CHICAGO • HUNTSVILLE
LOS ANGELES • McLEAN • PALO ALTO • SANTA BARBARA • SUNNYVALE • TUCSON

P.O. Box 2351, 1200 Prospect Street, La Jolla, California 92037

Reproduced by
NATIONAL TECHNICAL
INFORMATION SERVICE
U S Department of Commerce
Springfield VA 22151

DISTRIBUTION STATEMENT A
Approved for public release;
Distribution Unlimited

CONTENTS

		Page
1.	INTRODUCTION	1
2.	CODE GENERALIZATIONS	3
	2.1 Inclusion of Sail	3
	2.2 Asymmetrical Problems	6
	2.3 Restart Capability	7
3.	COMPARISON WITH EXPERIMENT	8
4.	FAR FIELD CALCULATIONS	18
	4.1 FRI Far Field Code	18
	4.1.1 Summary of Progress	18
	4.1.2 Structure for Remaining Development	19
	4.1.3 Details of Code Structure	21
	4.2 Far Field Calculations of Surface Current	24
	4.2.1 Introduction	24
	4.2.2 Suggested Method	25
	4.2.3 Storage	28
	4.2.4 Conclusion	29
5.	FUTURE WORK	30

LIST OF FIGURES

Page

Figure 1. Specifications for comparison between INTERN and APL experimental measurements, including a computer plot of the computational mesh 11

Figure 2. Computer plot of density variance at a point 13.97 cm directly above body centerline 12

Figure 3. Computer plot of the density variance at a point 9.05 cm directly above the body centerline 13

Figure 4. Comparison of theory and experiment for the displacement of a fluid particle 14

Figure 5. Crosstrack surface current (U = .6 kts) 15

Figure 6. X/D = -4.00262E+0, X/D = 4.85482E+01, X/D = 8.79183E+01 16

Figure 7. X/D = 1.01304E+01, X/D = 1.53666E+02, X/D = 2.06028E+02 17

Figure 8. Block diagram of Flow Research internal wave code 23

1. INTRODUCTION

For the first quarterly report[1] we showed, in admittedly brief terms, how the code INTERN is constructed, and the physical basis for its content. In order to demonstrate the viability of the code some very preliminary calculations for both a towing tank and the real oceanic environment were performed.

During the quarter being reported upon here INTERN has undergone substantial evolution. Also, attempts at validation of the code have improved our understanding of the physical and numerical basis of the code a great deal. This validation process has included comparison with experiment, which is the ultimate test of any theoretical analysis. So far, this comparison against experiment has been very successful as the contents of this report will reveal.

In an effort to generalize the code, provision has been made for the inclusion of a sail for a submerged body. This work is also described below. In previous work it has been possible to assume left-right symmetry, but if one wishes to include shear currents or swirl, such a symmetry condition is not applicable. Initially INTERN was designed under the assumption of such symmetry. This is no longer necessary, and INTERN is now able to treat problems involving shear and swirl.

Also implemented in the code is the capability to make plots of the crosstrack surface current. Such plots are useful to obtain a pictorial idea of the surface pattern that is generated by the passage of a body below the surface.

Below we present details on the above subjects as well as a discussion of the sample calculations. A report from our subcontractor Flow Research on their far field code is also included.

Two problems in particular have us concerned about the proposed far field calculations: one problem is that of storage, which may likely be overcome; the other problem has to do with the modal approach itself. The modal approach, it seems to us, has virtue only if the number of modes that contribute is not large. That is, convergence is obtained with only a relatively small number of modes contributing. Present codes generally include twenty modes. Calculations by Selwyn[2] indicate that a significant fraction of the energy can reside in the higher modes, so that it is difficult to have confidence that twenty modes (or even substantially more) result in convergence. Included in this report are two possible suggestions for avoiding the difficulties with the modal approach presently used for the "analytical" calculations.

2. CODE GENERALIZATIONS

In this section we describe some of the changes and alterations which have been made to INTERN during this quarter. Naturally only the major changes are discussed here, since at this stage the code is still undergoing rapid development.

2.1 INCLUSION OF SAIL

Bodies which are designed for subsurface travel usually have a sail or conning tower placed near the top forward position of the body. While not making up a large fraction of the body volume, it is possible that such an object could contribute to or change the internal wave pattern generated by the body.

The body has so far been represented in INTERN by a simple source-sink combination (Rankine Ovoid). At a later stage more complicated distributions will be utilized to more precisely represent realistic body shapes. The sail[1] can be modelled in potential flow by means of a combination line source and line sink on the y = 0 plane (see the first quarterly report for the definition of our coordinate system) parallel to the z-axis.

Let m be the source (sink) strength per unit length in the z-direction; then

$$\vec{u}(\vec{x}) = \frac{m}{4\pi} \frac{dz'}{|\vec{x}-\vec{x}'|^3} (\vec{x}-\vec{x}')$$

where $\vec{x}'$ is the position vector to the line element dz'. In our case $\vec{x}' = (x_o, 0, z')$, so that

$$u(x,y,z) = \frac{m}{4\pi} (x-x_o) \int_{z'_a}^{z'_b} \frac{dz'}{\left[(x-x_o)^2 + y^2 + (z-z')^2\right]^{\frac{3}{2}}}$$

$$v(x,y,z) = \frac{m}{4\pi}\, y \int_{z'_a}^{z'_b} \frac{dz'}{\left[(x-x_o)^2 + y^2 + (z-z')^2\right]^{\frac{3}{2}}}$$

$$w(x,y,z) = \frac{m}{4\pi} \int_{z'_a}^{z'_b} \frac{(z-z')dz'}{\left[(x-x_o)^2 + y^2 + (z-z')^2\right]^{\frac{3}{2}}}$$

For the situation of interest here, there is a line source at

$$x_{10} = 2670 \text{ cm},$$

a line sink at

$$x_{20} = 1962 \text{ cm}, \text{ with}$$

$$z'_a = 502.9 \text{ cm}$$

and

$$z'_b = 960.12 \text{ cm}.$$

The source strength per unit length is

$$m = 176.19\, u_o .$$

These numbers can be checked by locating the stagnation point for the cylindrical streamline, $\psi = 0$, around the line source and sink, and are assumed to apply for a body 1006 cm at maximum diameter, and 9915 cm in length.

By performing the indicated integrals, one finds for the velocity field:

$$u(x,y,z) = \frac{m}{4\pi}\left[\frac{(x-x_{10})}{(x-x_{10})^2+y^2}\left(\frac{z-z'_a}{\left[(x-x_{10})^2+y^2+(z-z'_a)^2\right]^{\frac{1}{2}}} - \frac{z-z'_b}{\left[(x-x_{10})^2+y^2+(z-z'_b)^2\right]^{\frac{1}{2}}}\right)\right.$$

$$\left. - \frac{(x-x_{20})}{(x-x_{20})^2+y^2}\left(\frac{z-z'_a}{\left[(x-x_{20})^2+y^2+(z-z'_a)^2\right]^{\frac{1}{2}}} - \frac{z-z'_b}{\left[(x-x_{20})^2+y^2+(z-z'_b)^2\right]^{\frac{1}{2}}}\right)\right]$$

$$v(x,y,z) = \frac{my}{4\pi}\left[\frac{1}{(x-x_{10})^2+y^2}\left(\frac{z-z'_a}{\left[(x-x_{10})^2+y^2+(z-z'_a)^2\right]^{\frac{1}{2}}} - \frac{z-z'_b}{\left[(x-x_{10})^2+y^2+(z-z'_b)^2\right]^{\frac{1}{2}}}\right)\right.$$

$$\left. - \frac{1}{(x-x_{20})^2+y^2}\left(\frac{z-z'_a}{\left[(x-x_{20})^2+y^2+(z-z'_a)^2\right]^{\frac{1}{2}}} - \frac{z-z'_b}{\left[(x-x_{20})^2+y^2+(z-z'_b)^2\right]^{\frac{1}{2}}}\right)\right]$$

$$w(x,y,z) = \frac{m}{4\pi}\left[\left[(x-x_{10})^2+y^2+(z-z'_b)^2\right]^{-\frac{1}{2}} - \left[(x-x_{10})^2+y^2+(z-z'_a)^2\right]^{-\frac{1}{2}}\right.$$

$$\left. - \left[(x-x_{20})^2+y^2+(z-z'_b)^2\right]^{-\frac{1}{2}} + \left[(x-x_{20})^2+y^2+(z-z'_a)^2\right]^{-\frac{1}{2}}\right]$$

While the above formulae appear to be a trifle messy, they are really very simple to include in the subroutine for the potential flow. No parameter studies have been made to determine just how much influence the sail does have, but a sample calculation has been made which indicates that the sail does not contribute significantly to the internal wave generation. When time permits a careful comparison calculation can be made. Presently the sail is either included or excluded in the calculation by means of a control number ISAIL. Naturally, when the distances from the sail are such that the sail potential flow velocities are very small, this part of the overall potential flow is bypassed in the interest of computational speed.

The result that the sail does not contribute greatly to the internal wave generation can be understood physically by the fact that the fluid tends to go around the sail rather than be lifted up over it. There is some lifting near the top of the sail, but only for a short axial distance. Also perhaps one ought to use the theory developed for joined bodies, since it may not be possible to make a clear separation of the potential flow as we have done so far. This whole problem of a precise potential flow will be discussed more fully at a later date. In any case a careful parameter study needs to be done before a firm conclusion about the influence of a sail is drawn.

2.2 ASYMMETRICAL PROBLEMS

The original design for INTERN included the assumption of left-right symmetry for the problems of interest. This assumption is unduly restrictive and a considerable effort was undertaken to eliminate this particular restriction. A thorough debugging was essential to make certain that the code still gave correct results. It is now a relatively simple matter to run problems with or without left-right symmetry. A control number LSY $\neq$ 0 is used to designate asymmetrical problems.

WAKE SWIRL

Generally, a propeller imports a certain amount of angular momentum into the wake of a body. An efficient propeller will minimize the amount of energy that goes into angular motion. This angular or rotational motion in a wake is usually referred to as swirl. It would be convenient to have a model for swirl which could be readily used in a research tool such as INTERN. If one neglects the axial variations of swirl, so that the motion is strictly two dimensional, then the model presented in Ref. (3) for a simple type of eddy is probably an adequate one for our purposes.

Let us assume that the swirl then depends at any downstream time on only the radial distance from the track. If u_o is the orbital velocity, then the swirl motion is described by

$$u_o = \frac{Ar}{2\sigma t^2} e^{-r^2/4\sigma t}$$

where σ will be taken as a turbulent viscosity, A is a constant, and t the downtrack time from the propeller. Both the constant A and the initial distribution can be obtained from the assumption for the initial energy associated with the swirl motion, which should be something less than 10% of the initial wake energy (potential energy).

No calculations have yet been made using the above model for the swirling motion behind a propeller with INTERN. Such calculations would be very easy to perform if ARPA so desires. It is felt that it would be best to first validate the code without too many effects included so that any problems encountered can be identified. When confidence is assured that the code gives correct answers, then we can readily proceed to include these extra effects. For example, we should be satisfied that the turbulence model is satisfactory before straining its credibility in the presence of current shear and swirl. Also, it is important that the far field be computed satisfactorily before we attempt to refine the physical content of the code. Another point is that the presence of current shear requires the nonlinear terms or special treatment this will effect the far field calculations.

2.3 RESTART CAPABILITY

It is highly desirable that it be possible to restart INTERN in case one wishes, on any particular calculation, to compute further downstream. This bookkeeping task has been accomplished, and it is possible now to perform such a restart. Many features of this nature must be included to make INTERN a convenient user's code.

3. COMPARISON WITH EXPERIMENT

As part of the validation process for INTERN it is important to compare the code results not only with other types of calculations, but with experiment where possible. The turbulence model had been compared with Naudascher's data in the previous quarterly, but during this last quarter, an effort was made to check INTERN against experimental results taken at APL.

Basically, the APL experiment consists of a tank containing stratified water through which a self-propelled 12:1 slender body is run. The body, except for the absence of a sail and trim planes, is shaped realistically. In our calculation we utilized a Rankine Ovoid with the same maximum diameter and the same length as the APL model. The specifications for the comparison are shown in Fig. (1) along with a picture of the computational mesh. The stratification was assumed linear in the calculation, whereas the experiment showed some deviation, particularly very near the top and the bottom.

The calculation was run twice, once without the wake, i.e., utilizing body generated waves only, and again allowing for both body and wake generated waves. As in our comparison with Naudascher, the wake is initiated four diameters behind the body.

Figures (2) and (3) show computer plots of the density variation for the case of body waves only. Due to the variable time-step in the wake calculation we do not have comparable plots when the wake is present. This plot could easily be added for the wake also. For the actual comparison with experiment, the numbers were printed out and hand plotted on the same graph paper used for the experiment.

Figure (4) demonstrates the comparison that was obtained between theory and experiment which appears to be quite good. Although we understand there is more complete data being taken, the experimental data we have plotted becomes much less reliable beyond 60 diameters downstream. The calculation was first run using data assuming the same turbulence profile that was used to compare

with Naudascher's data. This profile made the calculation become out of phase with experiment beyond 40 diameters downstream. By using a value q_o based on $|u'| = .087\ u_o$, in close agreement with the FRI and VPI data for momentumless propeller wakes (Naudascher used a jet), the phase of the calculation agrees very well with the APL experiment.

In the calculation shown in Fig. (4) a completely mixed wake was assumed, although various runs using widely different values for the mixing had only very small effect. Presumably a greater effect would be seen downstream. A plot of the crosstrack surface current downstream of the body is shown in Fig. (5). This plot is made by connecting values of the surface velocity v_y in the y direction at many axial positions. The extreme smoothness of the plot shows that the numerical procedures in the code work very well indeed. Figures (6) and (7) show some velocity vector plots of the flow field in the tank. We observe that beyond 100 diameters downstream there are severe top and bottom reflections in the tank.

There are several points that should be made about this comparison between theory and experiment. First there is the question of the difference in body shapes between that used in the experiment and of the Rankine Ovoid assumed in the calculation. This could account for the difference observed in the region near the body. Additionally, while the experimental angle-of-attack is limited to .004 radians it is still possible that such an angle-of-attack could help explain any variance between theory and experiment. Both of these effects can be taken account of in INTERN. Particularly, the angle-of-attack question should be addressed for very practical reasons. We have given some thought to this question and are confident that this can be included in the primary potential flow. Another interesting question is the point at which the wake should be initiated. If this point is chosen poorly then the choice will have an adverse effect upon the computed phases of the internal wave field. Presently INTERN initializes the wake at four diameters - which might be too far. This point should be investigated more thoroughly. Another

point in regard to our turbulence model is the fact that we likely must allow for the suppression of the vertical turbulent velocity fluctuations w', i.e., our model for turbulence should be anisotropic. Such a model is included in WAKEVM, and can be incorporated in INTERN. There is evidence that within a Väisälä period the turbulence is strongly anisotropic.

The calculation for the APL tank has been carried farther downstream - to 210 diameters (4.5 Väisälä periods), but as yet we have no data to compare it to. This run was made utilizing realistic density profiles. Hopefully we will be able to make comparisons with data in the next quarterly report. Such a comparison will also show the adequacy of our present turbulence model farther downstream.

At the present time we are making calculations on the density profiles sent to us by Dr. Phil Selwyn. So far we have run three of the cases and have encountered absolutely no difficulty in making these runs. The difficulty for INTERN (which we trust is very temporary) is of course the far downstream or far field calculations which we discuss in more detail in the next section. Since INTERN is not susceptible to the same kinds of problems that these test problems were intended to show we do not plan, in the interest of economy, to run all the test problems.

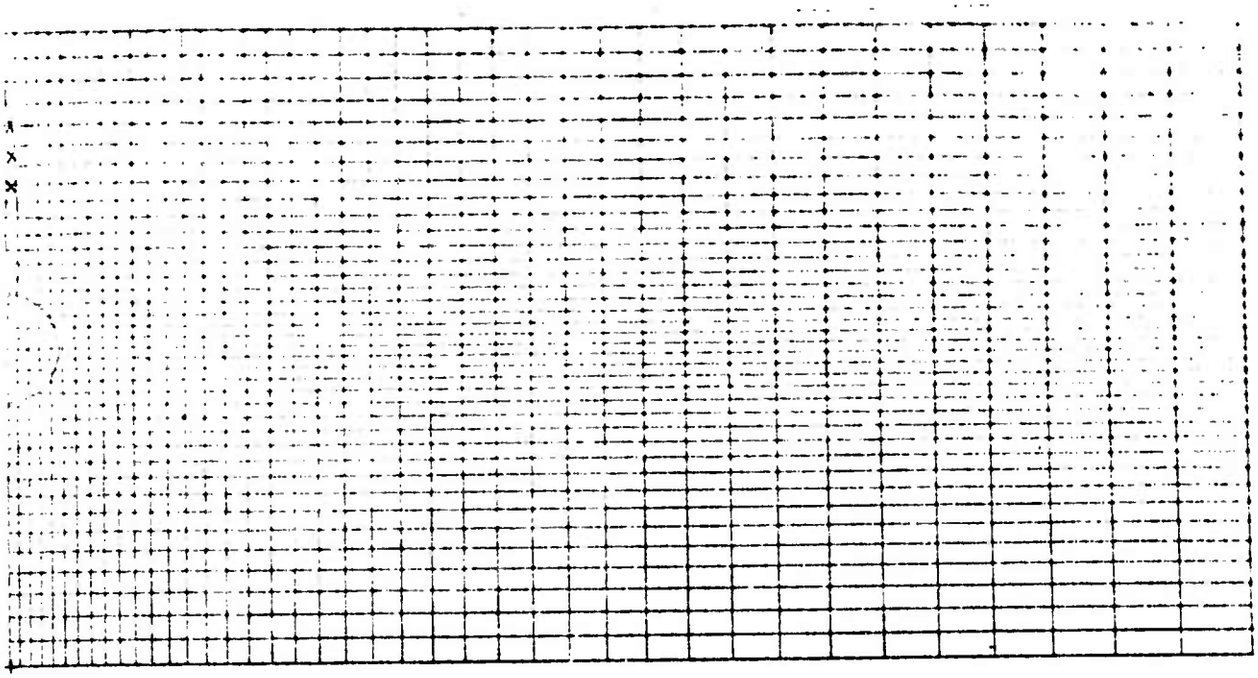

MINIMUM CELL SIZE	0.75 cm
MAXIMUM DIAMETER OF OVOID	7.62 cm
TANK HALF-WIDTH	90.5998 cm
TANK HEIGHT	45.8086 cm
STRATIFICATION	$2.7591\delta \otimes 10^{-4}$/cm
VÄISÄLÄ FREQUENCY (AVERAGE)	0.52 rad/sec

COMPUTATION POINTS: (INDICATED ABOVE) $\begin{Bmatrix} Z3 = 11.94 \text{ cm} \\ Z2 = 14.23 \text{ cm} \\ Z1 = 17.22 \text{ cm} \end{Bmatrix}$ measured from centerline

ACTUAL PROBE LOCATIONS: $\begin{Bmatrix} Z3 = 11.43 \text{ cm} \\ Z2 = 13.97 \text{ cm} \\ Z1 = 16.51 \text{ cm} \end{Bmatrix}$

LENGTH OF OVOID	91.44 cm
NO. VERTICAL CELLS	38
NO. HORIZONTAL CELLS	40
BODY SPEED	29.464 cm/sec

Figure 1. Specifications for comparison between INTERN and APL experimental measurements, including a computer plot of the computational mesh.

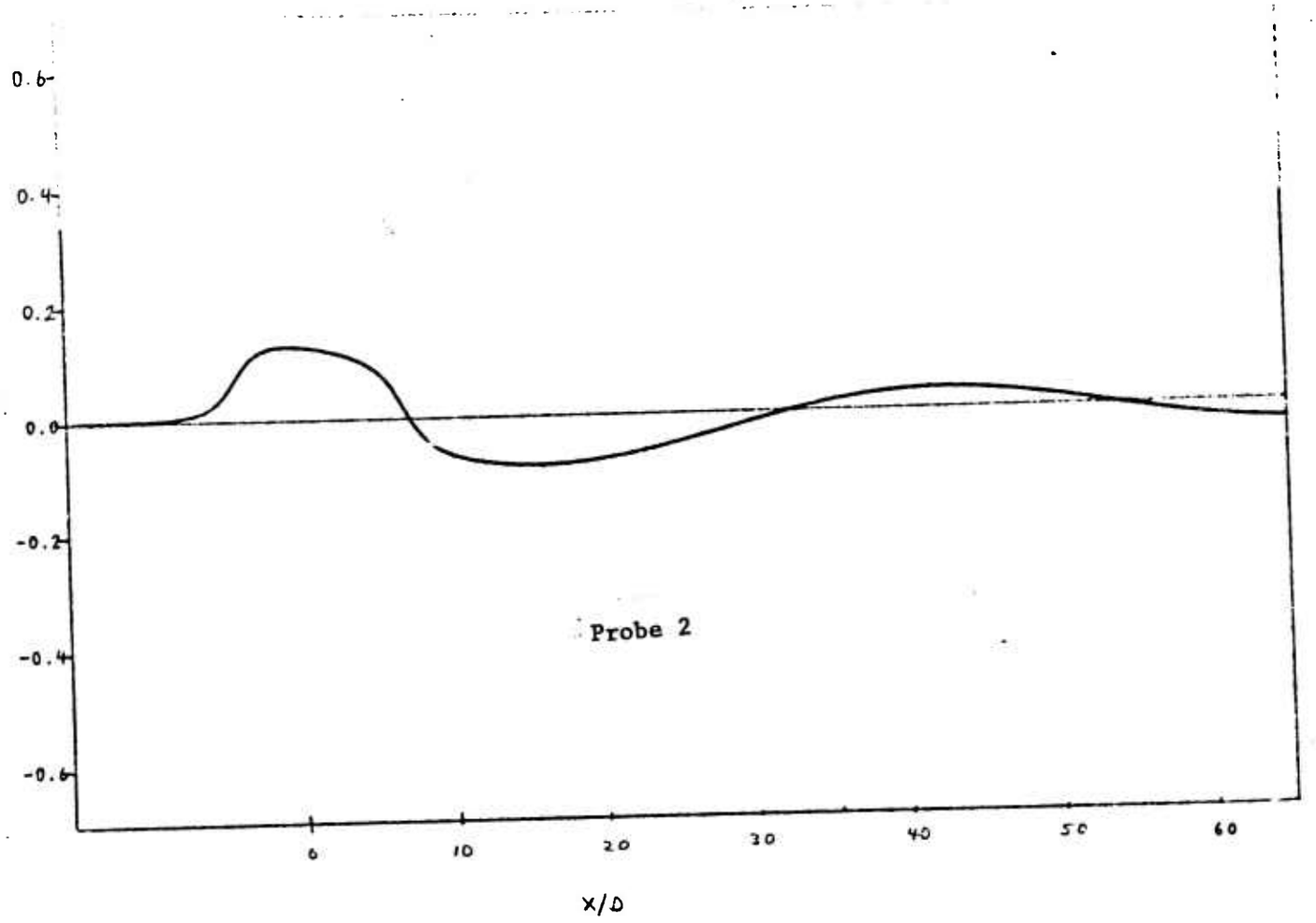

Figure 2. Computer plot of density variance at a point 13.97 cm directly above body centerline (body only).

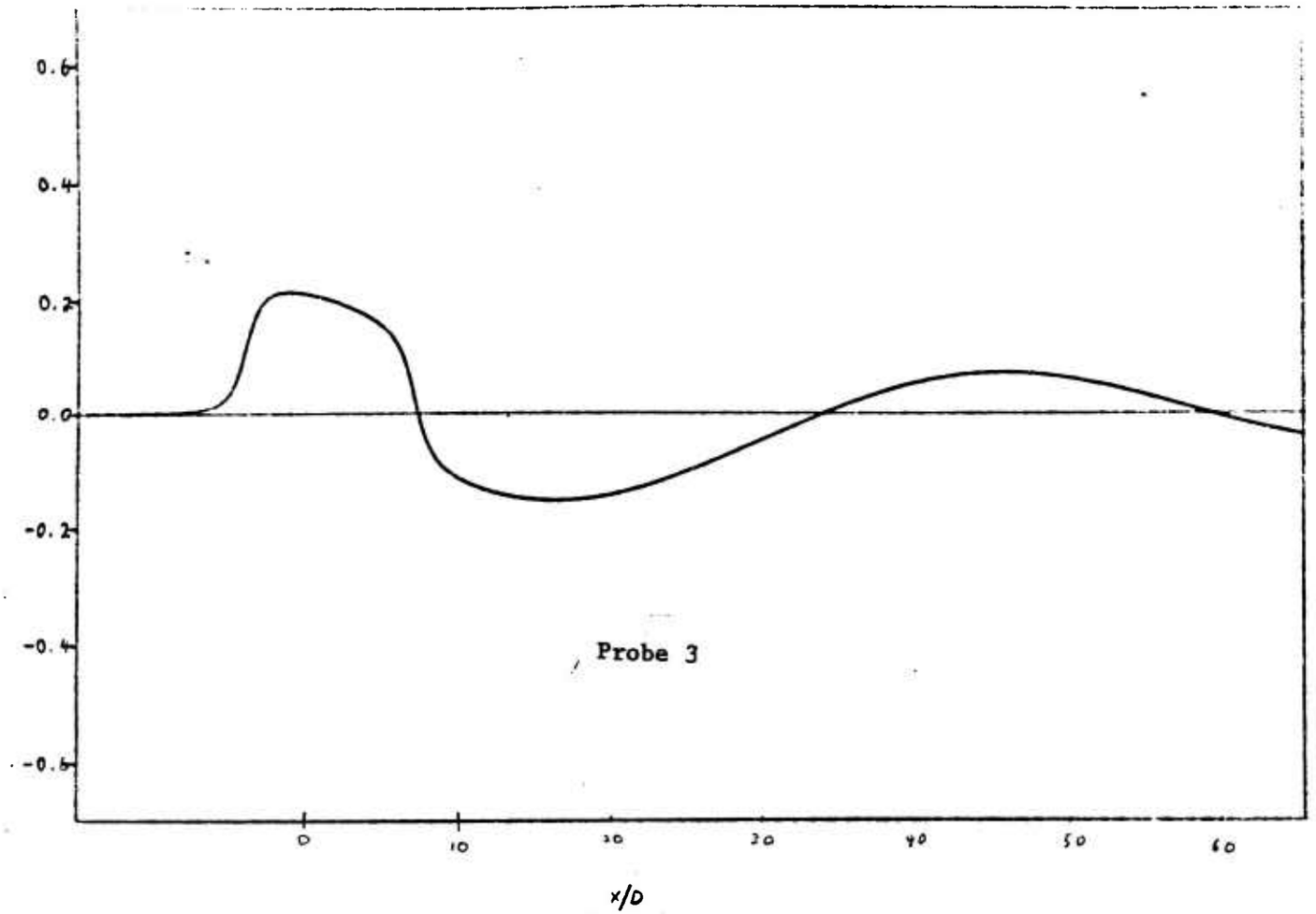

Figure 3. Computer plot of the density variance at a point 9.05 cm directly above the body centerline (body only).

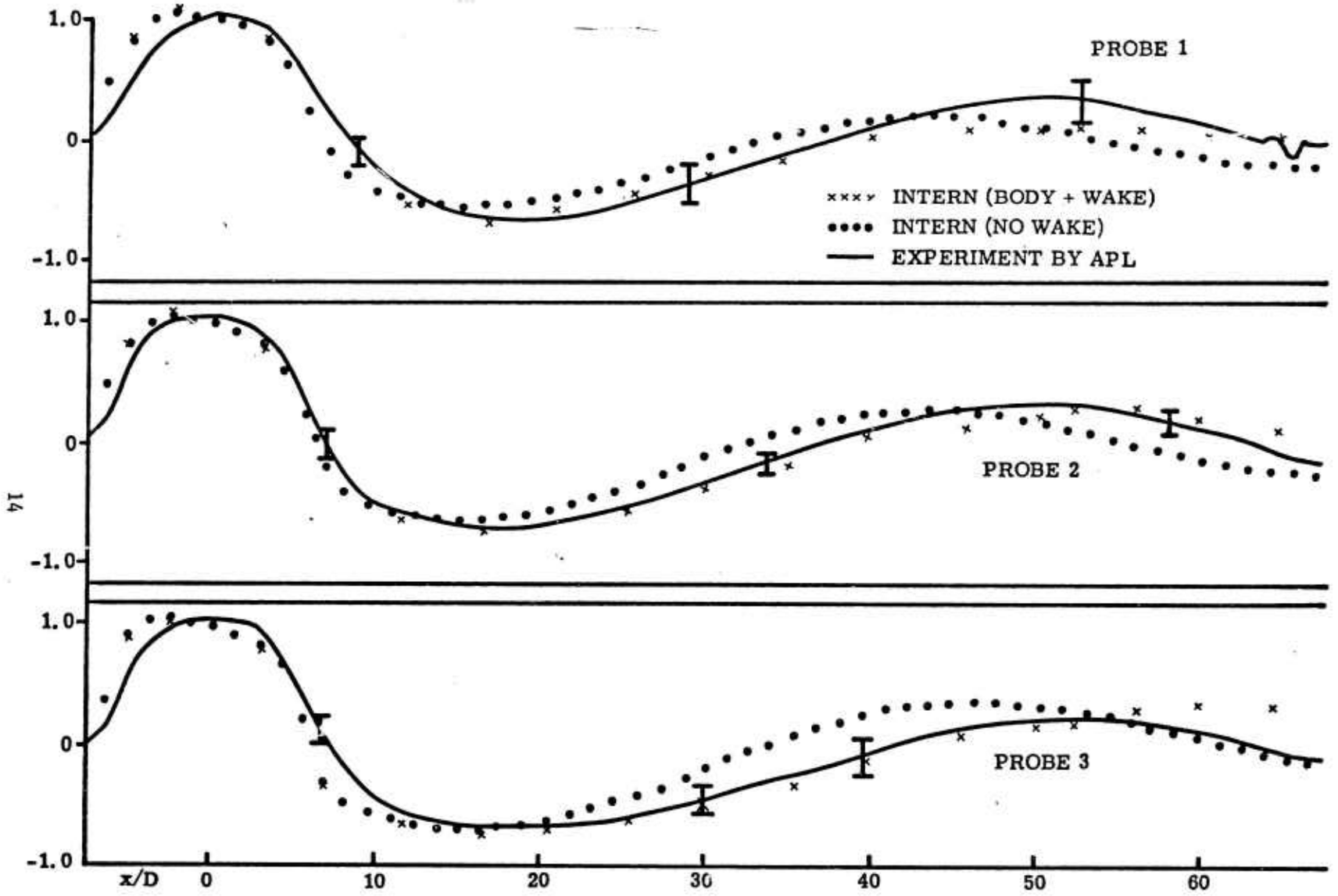

Figure 4. Comparison of theory and experiment for the displacement of a fluid particle.

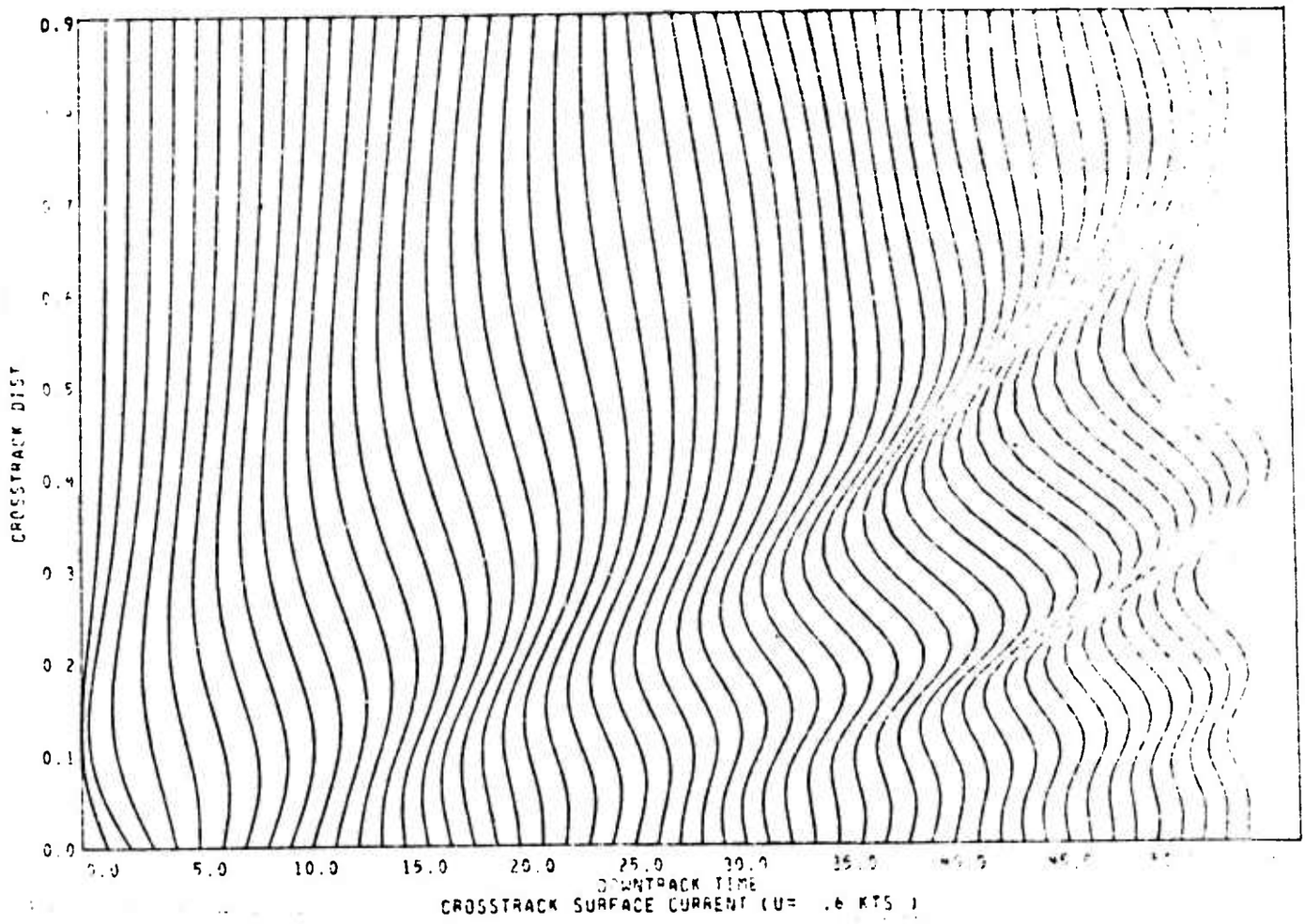
0.9
0.0
0.1
0.2
0.3
0.5
5.0
10.0
15.0
20.0
25.0
CROSSTRACK DIST
DOWNTRACK TIME
CROSSTRACK SURFACE CURRENT (U= .6 KTS)

Figure 5.

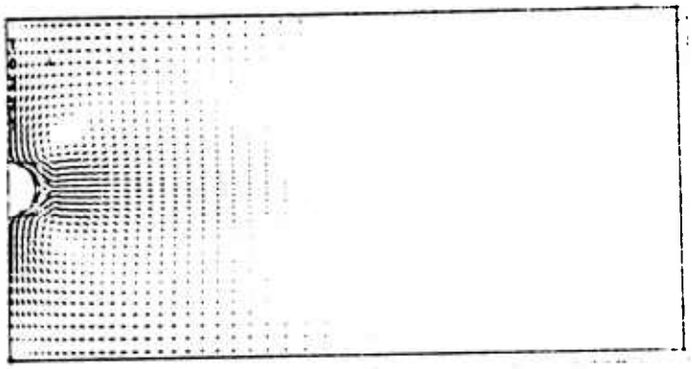

X/D = -4.00262E+0

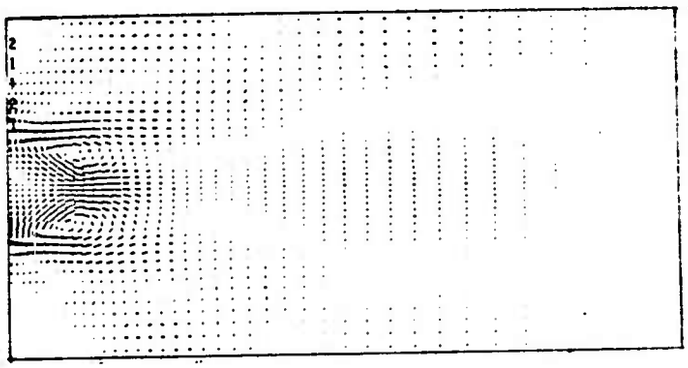

X/D = 4.85482E+01

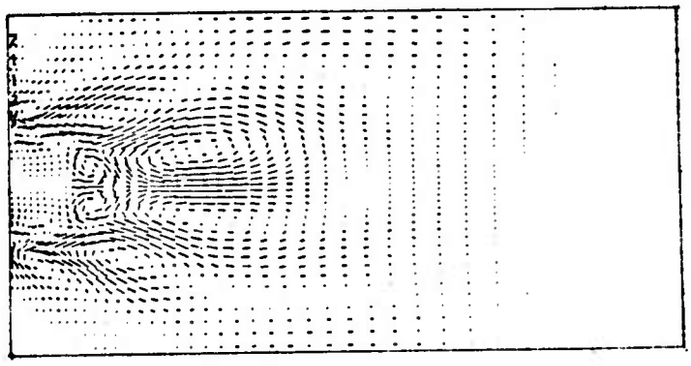

X/D = 8.79183E+01

Figure 6.

Velocity plots for APL experiment.

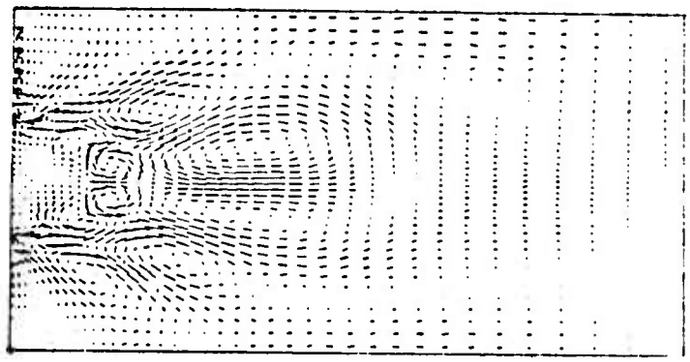

X/D = 1.01304E+01

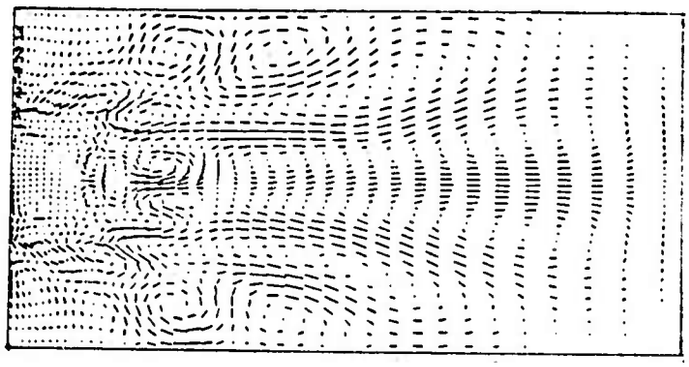

X/D = 1.53666E+02

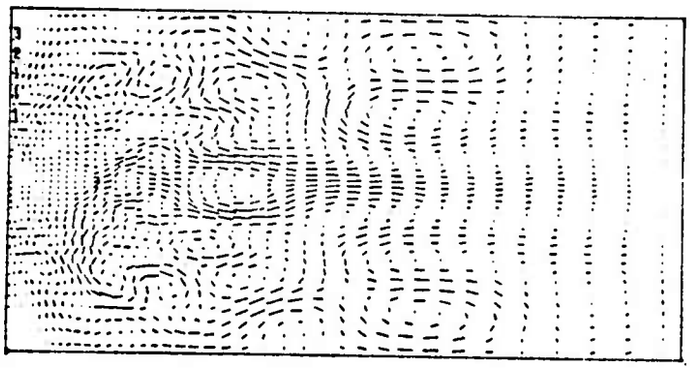

X/D = 2.06028E+02

Figure 7.

Velocity plots for APL experiment.

4. FAR FIELD CALCULATIONS

In this section we discuss the situation regarding the far field calculations. Below in Section 4.1 is a report from our subcontractor Flow Research.

As mentioned in the introduction, the far field approach taken by Flow Research, and used by others for these kinds of calculations, namely the modal approach, has us sufficiently concerned that we are looking at other methods for far field calculations. In particular, the questions of completeness, convergence and computer storage are the main items of interest. In Section 4.2 we present an alternative analytical approach which is being considered. This approach was suggested by P. Roache at SAI, and is a variation upon the FRI method.

Another method being considered is analogous to the Region I solution in INTERN. This method has the advantage of being simple, and of being accurate. Basically, the method consists of turning off the turbulence and the potential flow solutions of Region II, allowing more storage capacity and a great increase in speed. Another method is also being studied, but it is too preliminary to report at this time.

4.1 FRI FAR FIELD CODE

4.1.1 Summary of Progress

During this report period, a link with the LBL computing facility has been established, the basic elements of the FRI internal wave code have been developed or acquired and successfully tested, and the structure for the remaining development has been defined. The current version of the code calculates the internal waves generated in an ocean or a fluid with sidewalls by a moving source-sink disturbance. It has been partially validated by comparisons with computations based on the work of Smithmeyer and Pao[4] in which a constant-N fluid is assumed. Validation for more general stratifications is in progress.

The source-sink calculation is based on the following expression:

$$\psi(x,y,z) = -\frac{2}{\pi}\frac{\nu_o}{U}\int_o^\infty \sum_n \frac{\sin\left(\frac{\beta\ell}{2U\gamma_n}\right)\sin\left(\frac{\beta x}{U\gamma_n}\right)}{\gamma_n^2}\phi_n'(-h,\beta^2)\phi_n(z,\beta^2)\cos\beta y d\beta \quad (1)$$

where ψ is fluid displacement and definitions of the other symbols can be found in Ref. (5). For Eq. (1) and in general, our wave code utilizes Milder's[6] subroutines for computing the eigenmodes of the equation

$$\frac{d^2\phi}{dz^2} + \beta^2\left(\frac{N^2}{\omega^2} - 1\right)\phi = 0 ,$$

subject to the boundary conditions

$$\phi(0) = \phi(-H) = 0 .$$

Selwyn's[7] improvements to Milder's routine, ZMODES, have been included. In our use of the discrete Fourier transform to evaluate inverse integral Fourier transforms (see Eq. (1) and Ref. (8)), we use procedures for calculating real sine and cosine transforms described by Cooley[9] to take advantage of the usual circumstance that the integrand is a real, odd or even function, such as in Eq. (1). The speed of our FFT algorithm is thus increased by a factor of 4.

4.1.2 Structure for Remaining Development

Early in the development of our code, we decided to lead up to the full complexity of obtaining the flow downstream of a plane of initial data by solving a sequence of simpler problems. This approach facilitates the job of validation, since each block of code, starting with the basic eigenmode and Fourier transform routines, can be independently tested.

Having solved the source-sink problem, the next step in our code development plan is to solve the initial plane problem given an initial distribution of fluid displacement (the wake collapse problem). We will first choose a displacement distribution which can be analytically Fourier transformed, such as

$$\Psi(y,z) = \Psi_o \frac{z}{L_z} \exp\left(-\frac{y^2}{L_y^2} - \frac{z^2}{L_z^2}\right)$$

where L_z and L_y are length scales. The resulting expression for displacement downstream of the initial plane is

$$\psi(x,y,z) = -\frac{1}{2\pi}\int_{-\infty}^{+\infty} e^{i\beta y} \sum_n \frac{\cos\alpha_n x}{\gamma_n^2} \phi_n(z,\beta^2) \int_{-H}^{o} \phi_n(\hat{z},\beta^2)\left[\frac{d^2}{d\hat{z}^2}\Psi^* - \beta^2\Psi^*\right] d\hat{z}$$

where Ψ^* is the transform of the initial data. This version of the code will be validated by comparing its results to those of Dugan[10] and Young[11]. We then will allow for the specification of an initial grid of displacement data requiring numerical transformation. Finally, we will solve the full initial plane problem by permitting the specification of an initial grid of the perturbations w, v, ρ, and p. The first of the above steps will require a z-integration procedure, the second step, in addition, will require a procedure to numerically Fourier transform the initial data, and the last step will require a generalization of these procedures.

An important option to be added to the code as time permits is the use of a stationary phase approximation when the distance downstream becomes so large that the discrete transform becomes inefficient because of wake spreading and increasingly high oscillation frequencies in the lateral spectrum. In fact, the stationary phase approximation becomes more accurate as the discrete transform becomes more inefficient. For the source-sink problem the stationary phase result for the integral of the n^{th} mode is

$$\psi_n \sim \sum_s \frac{1}{2}\left[\frac{2\pi}{\frac{x}{U}\left|\frac{d^2}{d\beta^2}\left(\frac{\beta}{\gamma_n}\right)\right|}\right]^{\frac{1}{2}} \frac{\sin\left(\frac{\beta\ell}{2U\gamma_n}\right)}{\gamma_n^2} \phi_n'(-h)\phi_n(z) \times$$

$$\times \sin\left[\beta\left(\frac{x}{U\gamma_n} - y\right) + \operatorname{sgn}\frac{d^2}{d\beta^2}\left(\frac{\beta}{\gamma_n}\right)\frac{\pi}{4}\right]\Bigg|_{\beta=\beta_{ns}}$$

where β_{ns} is a solution to

$$\frac{d}{d\beta}\left[\beta\left(\frac{\cos\theta}{U\gamma_n} + \sin\theta\right)\right] = 0 .$$

For additional details on the current status and further development of the code, see Section 4.1.3 of this report.

A final note is that many of the details of the interfacing with the near wake calculation of SAI have been worked out. Most importantly, it has been decided to keep the SAI and FRI codes essentially separate. The FRI code will obtain the initial data that it requires from a tape generated by the SAI code. This modular approach avoids the complication of using overlays, thereby increasing the flexibility and transferability of the combined SAI-FRI programs.

4.1.3 Details of Code Structure

Figure 8 is a block diagram of the FRI internal wave code. Existing modules are denoted by solid lines, whereas dotted lines are used to indicate future development. Each arrow corresponds to the calling of a subroutine. The modules are described below:

EXISTING ROUTINES

FRIWAC	- controls I/O and program flow
TCLINE	- sets up the array defining N(z)
SPLINES	- computes cubic spline coefficients
SPLINE	- calculates interpolated values using coefficients computed by SPLINES
GRAPH	- produces printer plots
ZMODES	- controls calculation of dispersion relations and eigenfunctions
EIGENVL	- obtains convergence of eigenvalue - eigenfunction iteration procedure

EIGENFN - uses finite differences to compute trial eigenfunctions

FINT - does third order interpolations in conjunction with GRAPH

CMODE - controls wave field calculation

SSINV - computes contribution to wavefield from source-sink disturbance using discrete Fourier transforms

SSNTRP - interpolates from eigenmode wave number grid to wave number grid required for discrete Fourier transforms

SIX - takes into account that the integrand (function of wave number) to be transformed is even

FIVE - takes into account that the integrand is real

EXSET - sets up exponentials for use of FFT algorithm

FFFT2 - uses FFT algorithm to compute discrete Fourier transform

FUTURE ROUTINES

IPLANE - will Fourier transform a grid of data given at initial plane

ZING - will compute z-integrals from transformed initial plane data

IPINV - will compute contribution to wave field from initial plane data using discrete Fourier transforms

SSSPV - will compute contributions to wave field from source-sink disturbance using method of stationary phase

IPSPV - will compute contributions to wave field from initial plane data using method of stationary phase

CSPV - will calculate stationary phase points

PLTFLD - will provide plots of the wave field

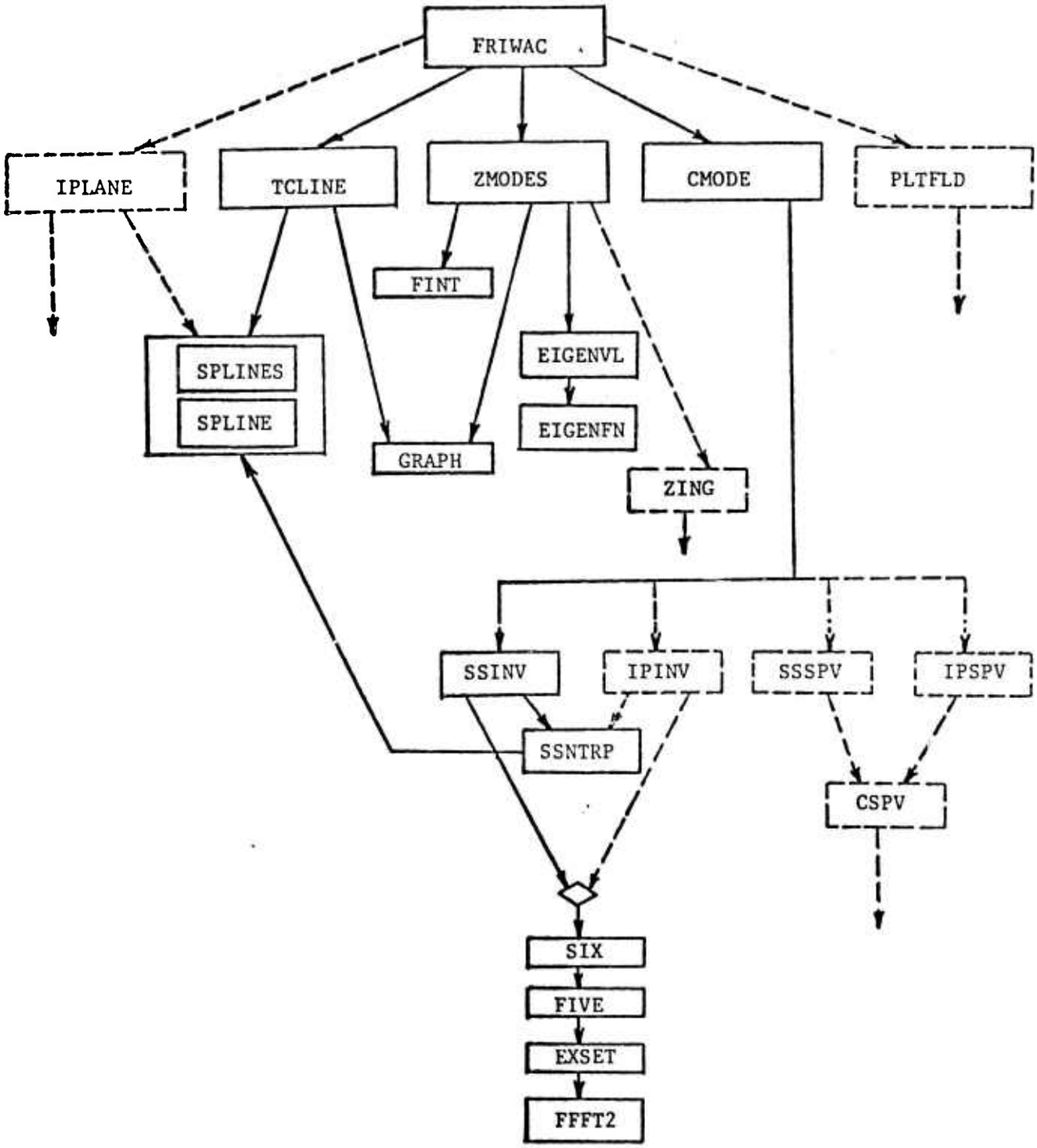

Figure 8. Block diagram of Flow Research internal wave code. Solid lines indicate current status, dotted lines denote future development.

4.2 FAR FIELD CALCULATIONS OF SURFACE CURRENT

In this section we describe an alternative approach to the far field analytical calculations being undertaken by FRI. A method is described for calculating the far field surface current produced by a submarine and its wake. Initial data are provided at a vertical plane in the wake from either finite-difference calculations including turbulence modeling, or from an analytical potential-flow representation of the submarine. The method is based on numerical Fourier transforms in the cross-track direction, numerical Laplace transforms in the track direction, and a finite-difference solution in the vertical direction. Contrasted to a previously suggested approach, the present method involves no eigenfunction problem, and requires computer storage of only two-dimensional rather than three-dimensional arrays.

4.2.1 Introduction

Reference (1) is a progress report on the problem of calculating surface waves from a submarine or other moving submerged body, including turbulence in the near wake. The flow around the body and the near wake are to be obtained by finite-difference calculations, as described in Ref. (1), or may alternately be described with less accuracy by potential flow methods, as in Ref. (12). (However, the present method would not be restricted to a simple point source as in Ref. (12), but could use arbitrary distributions of sources, sinks, and circulation.)

The present report is concerned only with a method of calculating the far field, in which the flow is assumed inviscid. The theoretical development and notation is that of Ref. (1), but an entirely different approach is used for the solution of the linear problem of the far wake. The body moves along the positive x-axis (track direction), the y-axis is in the cross-track direction, and the z-axis is vertical, with $z = 0$ at the surface and $z = -H$ at the ocean bottom. The far field (Region III) begins at a distance x_2 behind the body. The velocity components of the fluid in (x,y,z) are (u,v,w), respectively. The most difficult part of the solution is to obtain $\partial w/\partial z$ at the surface.

The point of departure of the present method from that of Ref. (1) is Eq. (8) of Ref. (1), repeated here.

$$\frac{d^2}{dz^2}\hat{w} + \beta^2\left[\frac{N^2}{\alpha^2 U^2} - 1\right]\hat{w} = i\frac{\beta^2}{\alpha}W^*(\beta,z) + \frac{\beta}{\alpha}\frac{dV^*}{dz}(\beta,z) - \frac{g}{\rho_o}\frac{\beta^2}{\alpha^2}\frac{R^*(\beta,z)}{U} \equiv F(\alpha,\beta,z) \quad (2)$$

This is a complex ordinary differential equation in z for $\hat{w}(\alpha,\beta,z)$ where $\hat{w}$ is the doubly-transformed w-velocity component; $\hat{w}(x,y,z)$ has been Fourier-transformed in the y-direction, with the y-coordinate transforming to the real frequency domain β, and Laplace-transformed in the x-direction, with the x-coordinate transforming to the complex frequency domain α. $\bar{U}$ is the constant velocity of the body, and N=N(z) is the Brunt-Väisälä frequency given by

$$N^2 = \frac{-g}{\rho_o}\frac{d\rho_o}{dz} \quad (3)$$

where g is the acceleration of gravity and $\rho_o(z)$ is the density of the fluid. No restrictions on $\rho_o(z)$ or N(z) are required. On the right-hand side, the terms W^*, V^*, and R^* are the Fourier transforms in y of the initial values of w, v, and ρ at the plane $x=x_2$, i.e. $w(x_2,y,z)$ is Fourier transformed to $W^*(\beta,z)$, $v(x_2,y,z)$ to $V^*(\beta,z)$, and $\rho(x_2,y,z)$ to $R^*(\beta,z)$.

In Ref. (1) (pp. 24-25), it is proposed to solve this problem by expanding $\hat{w}$ in eigenfunctions which must be solved numerically. The question of the completeness of the set of eigenfunctions has been answered only tentatively (Ref. (1), pg. 26). The final solution still involves an integration in z and an inverse transform in β. The eigenfunction solution is anticipated to be the most time consuming part of the program, and will require 500,000 words of storage. (The CDC 7600 has 500,000 words of slow core storage and 70,000 words of fast core storage.)

4.2.2 Suggested Method

Here, we propose to avoid the eigenfunction problem entirely. For moderate-sized programs, we could do all calculations in fast core, with some buffering from slow core. No questions arise about the completeness of the eigenfunctions.

The essence of the suggested method is to solve Eq. (2) numerically, and to collapse a storage dimension out of the problem, without changing the actual dimensionality.

Equation (2) is an o.d.e. for $\hat{w}(\alpha,\beta,z)$. The right-hand side is three-dimensional, $F(\alpha,\beta,z)$, but only by α as a parameter. The complex quantities W^*, dV^*/dz, R^* are 2-D arrays in (β,z). We are interested only in $\partial\hat{w}/\partial z$ at the surface value of z=0, so we store a complex 2-D array $\partial\hat{w}/\partial z\big|_{z=0}=DZS(\alpha,\beta)$. We define a complex 1-D array TWAB(z) = $\hat{w}$. (We use the prefix T in a FORTRAN name to refer to a transformed quantity, as the caret ^ is used with an algebraic name.) For a pair of parameters (α,β), we solve the complex o.d.e. (2) for TWAB(z), requiring only 2-D storage in (β,z) on the right-hand side. The resulting z-derivative value at the surface, $\partial\hat{w}/\partial z$, is first evaluated by second-order one-sided differences on TWAB(z), and then stored as one element in $DZS(\alpha,\beta)$ for that pair (α,β) used in the solution. The process is repeated for other (α,β) pairs, sweeping out the soultion w=TWAB(z), and again requiring only 2-D storage, this time in (α,β), for DZS (α,β).

The solution of the o.d.e. (2) can be achieved directly by a tridiagonal solver (e.g., Appendix A of Ref. (13)), presuming that $0(\Delta z^2)$ centered differences are used. Higher-order methods such as $0(\Delta z^4)$ could also be readily incorporated, using a penta-diagonal solver for $0(\Delta z^4)$ equations, with the usual ambiguity about higher-order boundary conditions. The boundary conditions are $\hat{w}$=w=0 at z=-H and at z=0.

The final solution is obtained by reverse transforming the doubly-transformed variable $\partial\hat{w}/\partial z=DZS(\alpha,\beta)$. First, the β transform is achieved directly by using an FFT algorithm. Second, the α transform, which is a Laplace transform, is achieved by using FFT on modified data, as described by Cooley in Ref. (9). This reference also describes a method for determining the arbitrary parameter of the Laplace transform from considerations of accuracy and the maximum x-value desired. The solution gives $\partial w/\partial z(x,y)$ at the surface z=0.

The major advantage of this method is the avoidance of the eigenfunction solution and its associated storage problem. The only disadvantage is the requirement for a numerical inversion of a Laplace transform. This can be a delicate problem, but it is believed that the methods of Ref. (9) will permit accurate inversion. Other accuracy considerations are the same as the original method proposed in Ref. (1); particularly, we note the error associated with the assumption of periodicity in y, required by the use of a discrete Fourier transform in y. It is expected that this "aliasing" error will be small (Ref. (12), pg. 6).

In Ref. (1) (proposal, pg. 25) the "exact" boundary condition at the free surface z=0 is not the value w(x,y,o)=0 used above, but

$$w(x,y,o) + \frac{U^2}{g} \frac{\partial^2 \phi}{\partial x^2} (x,y,o) = 0 \tag{4}$$

It is stated that this condition "could be easily incorporated, if needed" in that solution method, but that its effect is expected to be quite small. In order to incorporate Eq. (4) in the presently suggested method, an over-all iteration procedure would be required. The entire procedure described above, with w(x,y,o)=0, would be used to obtain the k=1 iterate of the solution. Then the procedure would be repeated, using as a boundary condition, for the (k+1) iterate,

$$w^{k+1}(x,y,o) = - \frac{U^2}{g} \frac{\partial^2 \phi^k}{\partial x^2} (x,y,o) \tag{5}$$

Thus the incorporation of the "exact" boundary condition (4) at the free surface is seen to be possible but awkward in the presently suggested method.

Finally, surface velocities are solved from the following Poisson equation (Ref. (1), proposal).

$$\frac{\partial^2 \phi}{\partial x^2} + \frac{\partial^2 \phi}{\partial y^2} = - \frac{\partial w}{\partial z} \tag{6}$$

The velocity potential ϕ is related to the surface-wave velocity components by $u=\partial\phi/\partial x$ and $v=\partial\phi/\partial y$. The boundary condition at x_2 on the surface is set by the finite-difference solution to the near wake. (For small x_2 or large H, the turbulent near wake will not have "broken through" to the surface, and $\phi=0$ will apply at $x=x_2$.) At y=0, symmetry prevails, so v=0. For the other boundaries in y and x, the domain must be large enough to allow the use of approximate (computational) boundary conditions on ϕ or $\partial\phi/\partial n$, such as the undisturbed far-field condition $\phi=0$ or the less restrictive approximation $\partial\phi/\partial n=0$ (e.g., see Ref. (13), Section III-C). The solution to (3) would be achieved with any of several fast Poisson solvers (e.g., see Ref. (13), Section III-B-1,8,9). Since the number of node points in x and y will probably be powers of 2 (see below) and the boundary is rectangular, a good choice of methods is available; since FFT's and a tridiagonal solver are already used in the solution for $\hat{w}$, Hockney's method (Ref. (14)) is a natural choice for the Poisson solution. Finally, the desired surface-wave velocity components are determined by simple differentiation of the solution for ϕ, with $u=\partial\phi/\partial x$ and $v=\partial\phi/\partial y$.

As an alternative formulation, it was suggested in Ref. (1), pg. 22, to use the approximate equation

$$\frac{\partial v}{\partial y} = -\frac{\partial w}{\partial x} \tag{7}$$

at the surface. This simple initial-value problem for v(x,y) can be solved by marching outward in y from the symmetry plane y=0, where v(x,o)=0. This approximation is very easy to solve, and requires no further approximations of computational boundary conditions.

4.2.3 Storage

Since the complex arrays W^*, dV^*/dz, $R^*(\beta,z)$ are multiplied by complex coefficients in (2), it is necessary to have both the real and imaginary parts in core at the same time. However, the full complex array $DZS(\alpha,\beta)$ may be

stored in slow core, with the solution values buffered out, perhaps a line at a time, through a singly-dimensioned array DABZS(β). The fast core storage required at one time would be the 3 complex *-arrays, and the two-singly-dimensioned arrays TWAB(z) and DABZS(β).

The storage required would, of course, depend on the resolution required. For 256 points in the β (or y) direction and 30 points in Z, the *-arrays require 6 × 256 × 30 = 46,080 words, and the two 1-D arrays require 30 + 256 points = 286, for a total of 46,366 words. This leaves 23,634 words of fast core for the rest of the program. The inversion of DZS (α,β) and the Poisson solution for φ(x,y,o) must also fit into fast core, but these can sequentially share the locations of the *-arrays. For 64 points in the α (or x) direction, the complex array DZS (α,β) requires 2 × 256 × 64 = 32,768 words, which is less than the *-arrays and is easily accommodated. (BLAND COMMON would of course be used to utilize the array storage memory for compiling.)

Going entirely to the 500,000 words of slow core + 70,000 words of fast core, we could have tht three complex *-arrays in (β,z) dimensioned (1024 × 65), and the complex DZS (α,β) dimensioned (64 × 1024), giving a total of 6 × 1024 × 65 + 2 × 64 × 1024 = 399,360 + 131,072 = 530,432 words. This would leave 39,568 words of the combined fast core/slow-core memory for the rest of the program.

Other combinations will occur, but it is desirable that the number of discrete values in x and in y be powers of 2, in order to make best use of the speed of FFT routines. However, a single factor of 3 can also be allowed in some versions of FFT, without completely ruining the speed.

4.2.4 Conclusion

The suggested method appears to have advantages over that described in Ref. (1). No eigenfunction solutions are required, and only two-dimensional arrays need be stored. A numerical inversion of the Laplace transform is required. The suggested method is an alternate to the approach suggested earlier, and appears to be preferable to it.

5. FUTURE WORK

In the next quarter we intend to continue validation of the code, begin the preparation of a user's manual, and to concentrate on the development of the far field part of the code. We consider the completion of the far field capability to be the most important task facing us at the present time.

REFERENCES

1. Young, J. A., Chan, R. K.-C., Riley, J., and Ko, D., "Development of an Internal Wave Computer Code," SAI-74-598-LJ, 30 July 1974, Science Applications, Inc., La Jolla, California. See also Proposal, SAI-020-71-019-74.

2. Selwyn, P. A., Memorandum dated 7 October 1974, subject "Test Problems for Engineering Codes (U)," IDA HQ 74-16692, SAI/LJ D.C. 74:914, Confidential.

3. Dryden, Hugh L., Murnaghan, F. D., and Bateman, H., Hydrodynamics, Dover Publications, Inc., (1956).

4. Smithmeyer, M. G. and Pao, Y. H., 1973. "Analysis and Computation of Internal Waves Generated by a Moving Body in a Tank of Stratified Fluid," Flow Research Report No. 20, July, 1973.

5. Riley, J. J. and Ko, D. R. S., 1974b. "Internal Wave Generation in a Variable N Fluid: I. Formulation," Flow Research Note No. 49, July, 1974.

6. Milder, M., 1973. "User's Manual for the Computer Program ZMODE," R & D Associates, Report TR-2701-001, July, 1973.

7. Selwyn, P., 1974, Private communication.

8. Riely, J. J. and Ko, D. R. S., 1974a. "Development of an Internal Wave Generation Code (Region III: Far Field), Quarterly Progress Report," Flow Research Communication No. 18, July, 1974.

9. Cooley, J. W., Lewis, P. A. W. and Welch, P. D., 1970. "The Fast Fourier Transform Algorithm: Programming Considerations in the Calculation of Sine, Cosine and LaPlace Transforms," J. Sound Vib., 12 (3), 315-337.

10. Dugan, J. P., Warn-Varnas, A. G. and Piacsek, S. A., 1974. "Collapse of Partially Mixed Regions in Stratified Fluids," NRL Memorandum Report 2841.

11. Young, J., 1974. Private communication.

12. Milder, M., "Internal Waves Radiated by a Moving Source; Vol. 1 - Analytic Simulation," RDA-TR-2702-007, Feb. 1974, R & D Associates, Santa Monica, California.

13. Roache, P. J., Computational Fluid Dynamics, Hermosa Publishers, Albuquerque, New Mexico, 1972.

14. Hockney, R. W., "A Fast Direct Solution of Poisson's Equation Using Fourier Analysis," J. Association of Computing Machinery, Vol. 12, 1965, pg. 95.